RHEOLOGY OF MANTLE AND LITHOSPHERE INFERRED FROM POST-GLACIAL UPLIFT IN FENNOSCANDIA

W. FJELDSKAAR
Rogaland Research,
P.O. Box 2503,
4004 Stavanger,
Norway.

L. CATHLES
Cornell University,
Ithaca,
New York 14853,
USA.

ABSTRACT. The earth's response to glacial loading/unloading offers exceptional promise for the study of the physical properties of the lithosphere and mantle because aspects of the isostatic adjustment are very sensitive to mantle rheology and, to a lesser degree, lithosphere thickness. To determine these parameters the earth's response to deglaciation in Fennoscandia is modelled using a three-dimensional viscoelastic model in which the asthenosphere viscosity, mantle viscosity and lithosphere thickness are allowed to vary so that the maximum rate of present uplift matches its observed value. The ice profile is considered to be known. Comparison of tilting at particular locations and the pattern of present uplift and subsidence using this approach indicates that the lithosphere is less than 50 km thick, the mantle viscosity is 1.0×10^{22} poise and the asthenosphere is 75 km with viscosity 1.3×10^{20} poise.

INTRODUCTION

Movements of the earth's lithosphere in post-glacial time is generally assumed to be a consequence of mantle flow to achieve a new isostatic equilibrium following the redistribution of ice loads. The flow law relating mantle stress and strain rate may be linear (with strain rate proportional to the applied stress), non-linear, or a stress-dependent combination of the two. A linear flow law produces a unique response in areas peripheral to large ice loads if the viscosity of the mantle is reasonably uniform (Cathles, 1980). Since the deep flow response is similar to that observed, deep flow and linear rheology are indicated. In any case, a linear flow law has been assumed in most models used to simulate glacial uplift. A minor part of the observed uplift may be due to mantle phase boundary migration. This, however, is a process of importance only for loads applied for a million years or more (O'Connell, 1976). Despite issues of modelling, data on post-glacial uplift clearly provides very important

R. Sabadini et al. (eds.), Glacial Isostasy, Sea-Level and Mantle Rheology, 1–19.

information on the physical properties of the earth's mantle and lithosphere.

Fennoscandia is the classic area for studies of glacial isostasy. Fennoscandian data on the present elevation of past shorelines and the present rate of uplift relative to sea level have been used with geophysical models to determine the physical properties of the upper mantle and lithosphere for many years. From the very beginning there has been a dichotomy between channel flow ("bulge") models and deep flow ("punching") models, and this debate continues today.

The two conceptual adjustment end-members, "bulge" where loading produces large peripheral accumulations of mantle material squeezed from the load through a viscous channel, and "punching" (or deep flow) where the areas loaded or unloaded initially drag the peripheral regions with them in a sympathetic motion of much lower amplitude, were first articulated by Barrell (1914) and Daly (1934). The models were subsequently quantified in a channel flow model by Van Bemmelen and Berlage (1935) and a halfspace model of uniform viscosity by Haskell (1935). Both were shown to account equally well for the history of uplift in the central, most rapid uplifting, areas of Fennoscandia. Daly (1934) found no geological evidence for a channel bulge in peripheral areas (in fact saw just the opposits) and for this reason invented the "punching" hypothesis. Haskell showed that the lithosphere was not necessary to avoid peripheral bulges; deep flow with no lithosphere produced the punching effect needed by Daly.

More recently, Artyushkov (1971) and Mörner (1979) concluded that the uplift data suggests channel flow in a low viscosity asthenosphere situated between the rigid lithosphere and mantle mesosphere. McConnell (1968) showed by Fourier analizing the shape of the uplift pattern that the shorter harmonics decayed faster than the longer ones, suggesting flow in a 100 km thick asthenosphere of viscosity lower than 10^{21} poise. Cathles (1975) reconsidered McConnell's analysis and concluded the rapid decay of short wavelength harmonics required both a lithosphere and asthenosphere, and the straightening of the spectrum indicated deep mantle flow as well. A lithosphere was unlikely to alone cause the rapid adjustment of the shortest harmonics because it would support 90% or more of this load, not leaving significant decay to be observed. An asthenosphere and a lithosphere in combination could account for the decay spectrum nicely. An asthenosphere is also indicated if the zero uplift isoline in Fennoscandia is stationary with time (Cathles, 1980), as some have suggested.

The lithosphere has also been subject of much debate. Niskanen (1949) concluded at the end of a series of analyses that crustal effects dominate the recent Fennoscandian uplift. Jeffreys (1959) studied the deformation of an elastic crust by bending of a thin elastic sheet. His calculations suggest that large surface features such as large ice caps would attain isostatic equilibrium with little interfearance from the lithosphere. The current approach to including the lithosphere in isostatic adjustment calculations was pioneered by Walcott (1970). Based on long-term isostatic adjustment of small scale loads at various locations on the globe, Walcott concluded the flexural rigidity of the lithosphere ranged from 5×10^{22} to 4×10^{23} Nm, but the flexural rigidity over short timescales could be larger ($6\text{-}9 \times 10^{24}$ Nm). Gravity anomalies reflecting long term load support in Fennoscandia suggest a flexural rigidity of between 1 and 5×10^{24} Nm (Cathles, 1975). Based on a lower resolution (longer wavelength) analysis and a different global viscoelastic model (with non-adiabatic mantle density gradients), Peltier (1984) found evidence of a much

thicker (≈ 200 km) lithosphere.

Early models of linear viscosity on a flat, non-gravitating earth have been considerably improved by the work of O'Connell (1971, 1977), Cathles (1975 ,1980), Peltier (1974, 1980), which incorporate density changes in a spherical, gravitating, and cored earth with arbitrary viscosity distribution with depth. From the above discussion there is clearly little agreement in the present literature regarding the importance of the lithosphere and asthenosphere. In this context a high resolution study of Fennoscandia could be of particular interest. In this paper we will present a regional study of the Fennoscandian uplift data, involving calculations of the uplift response as a function of time to the observed deglaciation history. The calculations are based on a flat earth approximation with constant gravitation and adiabatic density gradients in a Newtonian mantle and an elastic lithosphere. The errors introduced by the flat earth approximation is not significant for a regional calculation. The advantage is high resolution calculation of the uplift response, and the ability to use local sea level observations to give a more stringent constraint on mantle viscosity and lithosphere rigidity than global calculations do.

UPLIFT DATA

The post-glacial uplift in Fennoscandia has been mapped by the following means:

1) Shoreline diagrams, showing the displacement and tilting of palaeoshorelines.

2) Shorelevel displacement curves, showing the vertical displacement at a certain point.

3) Repeated levelling, tide gauge and old water marks, recording the present uplift.

4) Gravity data, indicating the mass distribution and the remaining isostatic adjustment.

Unfortunately, much of the uplift data are not a direct measure of isostasy, but also include other effects of deglaciation (glacial eustasy, geoidal eustasy). In this study we have used data which is scarcely affected by effects other than glacial- and hydro-isostasy. The data types used are the shoreline diagrams (showing the tilting history of palaeoshorelines) and the present rate of uplift. It has been shown that the geoidal eustatic effect does not contribute significantly to the tilting (cfr. Fjeldskaar and Kanestrøm, 1979), and that the present rise of the geoid is less than 10% of the observed present land uplift of the area (Ekman, 1989). It is thus a reasonable approach to use the shoreline diagrams and the present rate of uplift as a direct measure of the deflections of the solid earth.

DEGLACIATION DATA

The deglaciation of the last ice age is relatively well established by observations of marginal moraines. The deglaciation history used here (Figs 1-5) is compiled by B.G. Andersen (Denton & Hughes, 1981). The glacial thicknesses is however a subject of discussion, because direct geological evidence of glacial thickness is meager. The glacial thicknesses used here is in accordance with the traditional view.

Fig. 1. The extent and thickness of the ice sheet at the last glacial maximum (20 000 BP). The contour interval is 400 m, except for the first (800m).

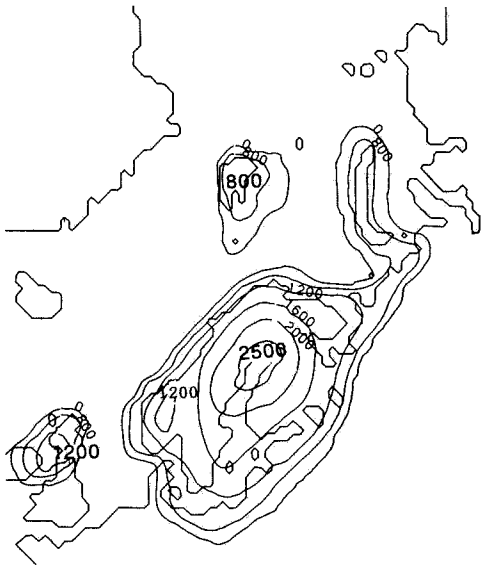

Fig. 2. The extent and thickness of the ice sheet at 15 000 BP. The contour interval is 400 m, except for the first (800m).

Fig. 3. The extent and thickness of the ice sheet at 11 500 BP. The contour interval is 400 m, except for the first (800m).

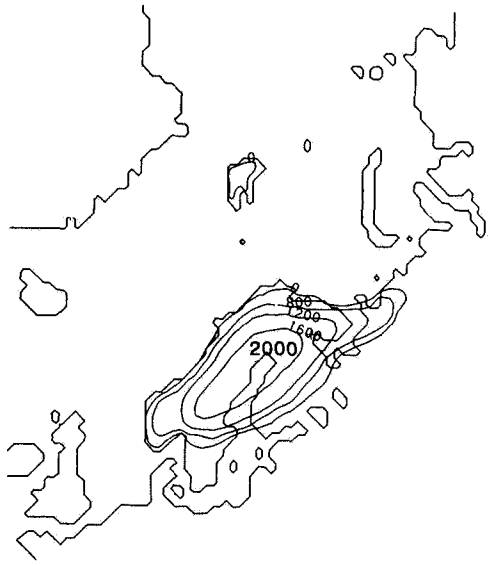

Fig. 4. The extent and thickness of the ice sheet at 10 500 BP. The contour interval is 400 m, except for the first (800m).

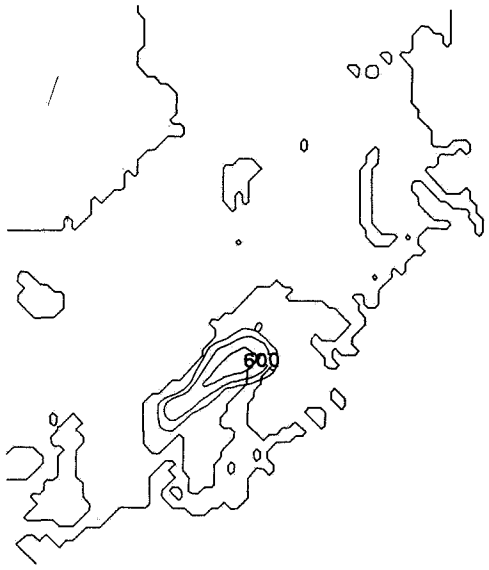

Fig. 5. The extent and thickness of the ice sheet at 9 300 BP. The contour interval is 200 m, except for the first (400m).

MODEL APPROACH

The earth is modelled by a non-spherical viscoelastic fluid in which the viscosity may vary with depth, overlain by a uniformly thick elastic lithosphere. With this flat earth model, we are able to treat the isostatic problem analytically, by the Fourier transform technique. The method used here is described in Cathles (1975), which we closely follow here (cfr. Appendix A, B). The mantle is treated as a layered Newtonian half-space, causing the rate of displacement to vary with wavelength of the Fourier load harmonics. The elastic lithosphere is treated as a low-pass filter, because loads of small size tend to be balanced by the lithosphere itself, and not by buoyancy. The lithosphere flexure also speeds the isostatic response.

HYDRO-ISOSTASY

Hydro-isostasy, the isostatic compensation due to changes in the water-load, is included in the calculations. The change in the water load is taken care of indirectly by the Fourier transform technique; it is assumed to be the DC component of the Fourier transformed ice load. The resulting glacial-eustatic curve (Fig. 6) is in accordance with what is generally believed reasonable.

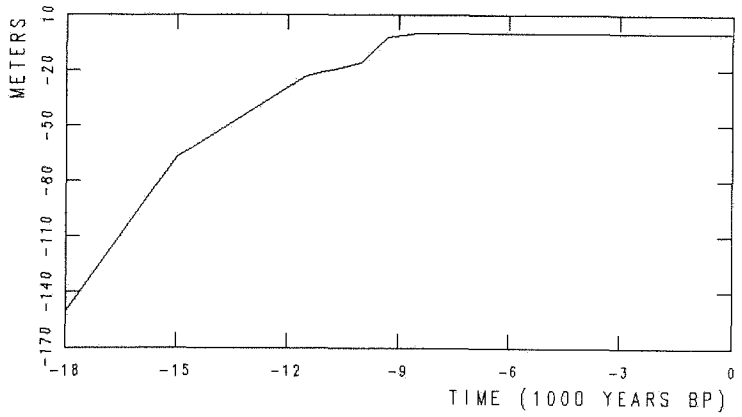

Fig. 6. Glacial-eustatic curve used in the calculations.

THEORETICAL VERSUS OBSERVED GLACIAL ISOSTASY

Glacial isostasy, movements of the solid earth to reestablish isostatic equilibrium during changes of the ice loads, is calculated by equation (5) based on the deglaciation history described above. The changes from one ice sheet configuration to the next is modelled with uniform speed.

PRESENT RATE OF UPLIFT

The observed present rate of uplift in Scandinavia relative to mean sea level increases from 0 mm/yr at the western coast of Norway to 9 mm/yr in central parts of Sweden (Fig. 7). To obtain the uplift of the crust relative to the geoid, the uplift rate has to be corrected for the eustatic sea level changes, which would, probably, add approximately 1 mm to the numbers given in Fig. 7.

The calculations of the present rate of uplift based on the reported deglaciation models show that the present uplift pattern is

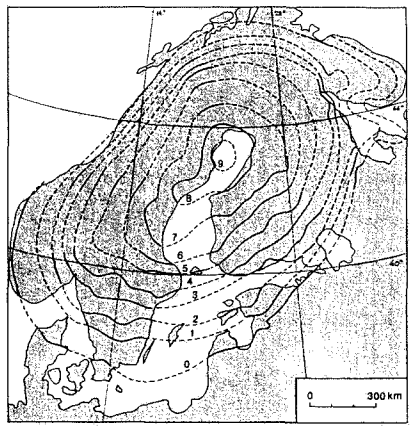

Fig. 7. Observed apparent rate of uplift in Fennoscandia (from Ekman, 1989).

mainly determined by the viscosity profile of the mantle. Changes of the lithosphere rigidity is causing only minor adjustments of this pattern.

The viscosity profile of the earth's mantle is found by comparing theoretical and observed pattern of the present rate of uplift. During the calculations the uplift rate of the centre is kept at 8.5-9.0 mm/years while the viscosity profile varies. A lot of possible mantle viscosity profiles turn out to be unrealistic because they give large discrepancies between theoretical and observed uplift rate in peripheral areas. On this basis the following viscosity profiles are ruled out as possible mantle rheologies:

1) Uniform viscosity mantle. To keep the centre uplift rate at 8.5 mm/years given a uniform mantle, the viscosity is 0.66×10^{22} poise. The uplift pattern shows large discrepancies from the observed data (cfr. Fig. 8). In particular, the peripheral subsidence has much larger amplitude than observed, and the spacing of the rate of uplift contours is not as uniform as required.

2) Two layered mantle with mantle viscosity $\eta > 1.3 \times 10^{22}$ poise. With asthenosphere thickness of 50-100 km (of viscosity 0.9×10^{20} poise) the theoretical peripheral uplift rates will be higher than observed, the zero uplift contour lies too far south and west (cfr. Fig. 9).

Thus it seems that the viscosity of the earth's mantle is somewhere between 0.66×10^{22} poise and 1.3×10^{22} poise, and overlain by a low viscosity asthenosphere. The best fitting model is the one that has a mantle viscosity of 1.0×10^{22} poise overlain by an asthenosphere of viscosity 1.3×10^{20} poise (Fig. 10). A plot of the relaxation time versus wavelength is shown in Fig. 11. The theoretical uplift response for 10 000 BP and 8 000 BP based on this mantle viscosity profile and a lithosphere rigidity of 10^{24} Nm are shown in Figs 12-13.

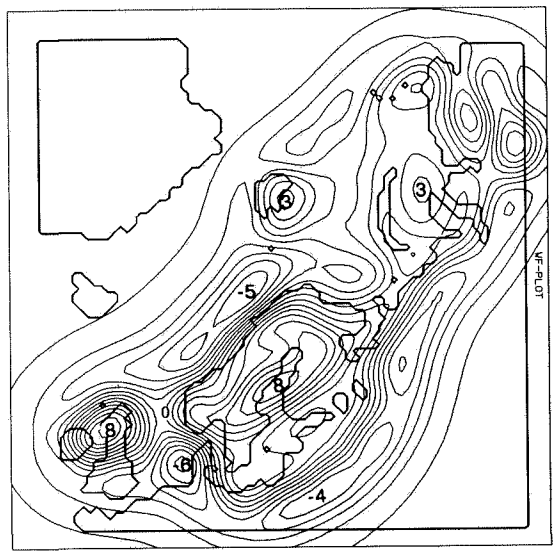

Fig. 8. Theoretical present rate of uplift based on a uniform mantle of viscosity 0.66×10^{22} poise and a lithosphere rigidity of 10^{24} Nm. Contour interval is 1 mm/year.

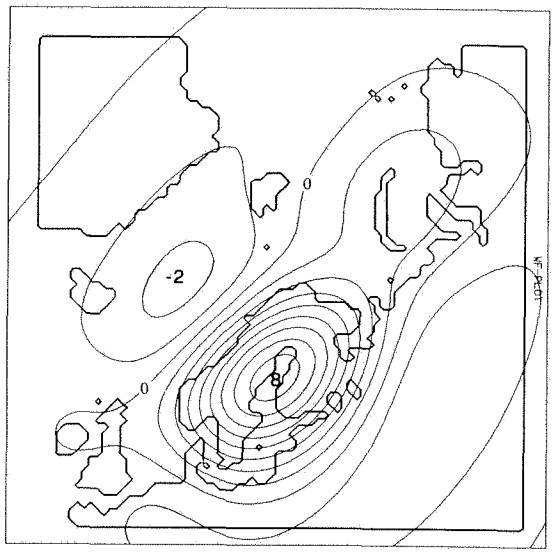

Fig. 9. Theoretical present rate of uplift based on a mantle of viscosity 1.3 x 10^{22} poise overlain by a 75 km thick asthenosphere of viscosity 0.9 x 10^{20} poise and a lithosphere rigidity of 10^{24} Nm. Contour interval is 1 mm/year.

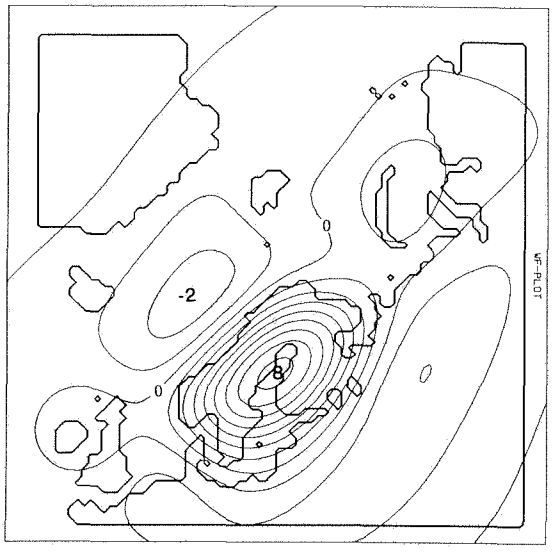

Fig. 10. Theoretical present rate of uplift based on a mantle of viscosity 1.0 x 10^{22} poise overlain by a 75 km thick asthenosphere of viscosity 1.3 x 10^{20} poise and a lithosphere rigidity of 10^{24} Nm. Contour interval is 1 mm/year.

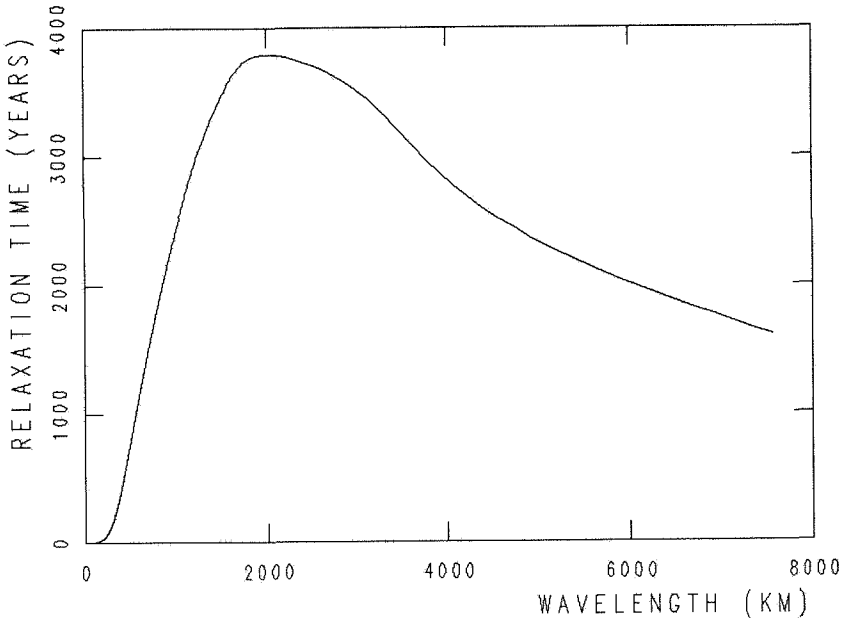

Fig. 11. Relaxation time versus wavelength for the preferred mantle rheology with a lithosphere rigidity of 10^{24} Nm.

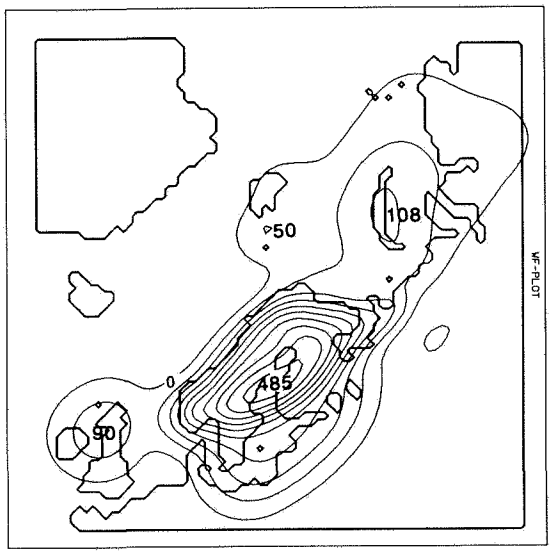

Fig. 12. Theoretical uplift response from 10 000 BP to present. Contour interval is 50 m.

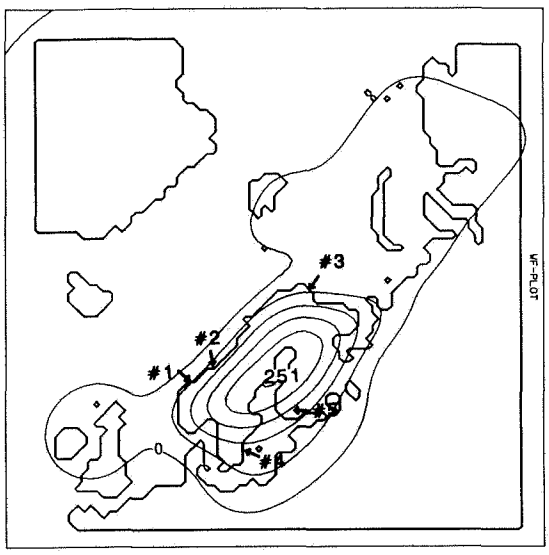

Fig. 13. Theoretical uplift response from 8 000 BP to present. Contour interval is 50 m.

SHORELINE TILTING HISTORY

As mentioned above the present rate of uplift is scarcely affected by the lithosphere rigidity; the uplift pattern calculated when using a rigidity of 10^{24} or 10^{25} Nm is hardly distinguishable. Information on the lithosphere rigidity is, however, revealed by the shoreline diagrams, which give the observed shoreline tilting versus time. Such curves are available, or may be constructed from local shorelevel displacement curves, for a number of localities in Fennoscandia, of which a few are selected here (locations; cfr. Fig. 13).

The theoretical vs. observed tilting as a function of time for the investigated areas (Figs 14-18) show that the lithosphere rigidity

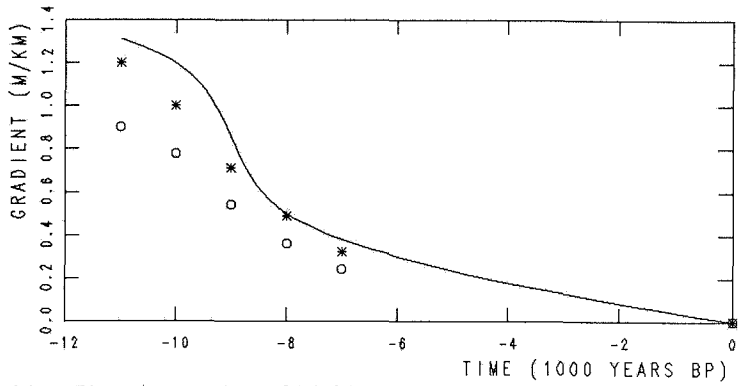

Fig. 14. The observed (solid line; from Svendsen and Mangerud, 1987) and theoretical shoreline tilting in the Sunnmøre area, central Norway (location 1 in Fig. 13). The calculations are done for flexural rigidity of 10^{24} and 10^{25} Nm, indicated by stars and dots, respectively.

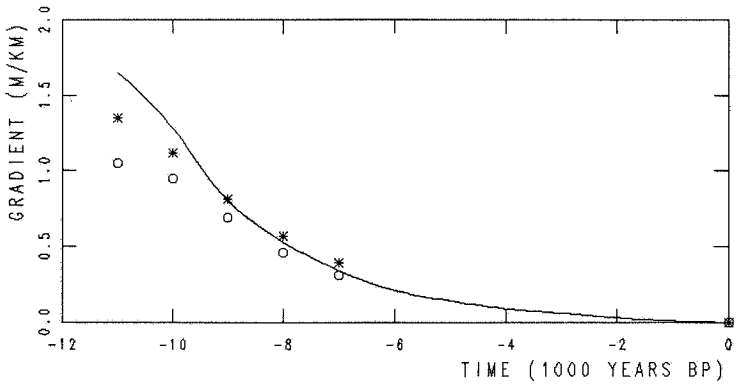

Fig. 15. The observed (solid line; from Kjemperud, 1981) and theoretical shoreline tilting in the Trøndelag area, central Norway (location 2 in Fig. 13). The calculations are done for flexural rigidity of 10^{24} and 10^{25} Nm, indicated by stars and dots, respectively.

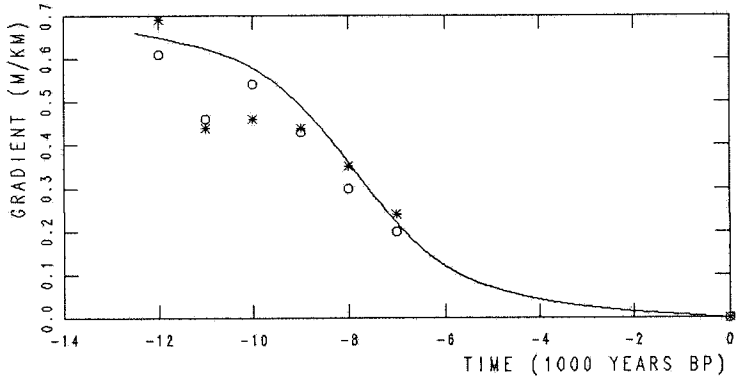

Fig. 16. The observed (solid line; from Marthinussen, 1974) and theoretical shoreline tilting in the Varangerfjord area, northern Norway (location 3 in Fig. 13). The calculations are done for flexural rigidity of 10^{24} and 10^{25} Nm, indicated by stars and dots, respectively.

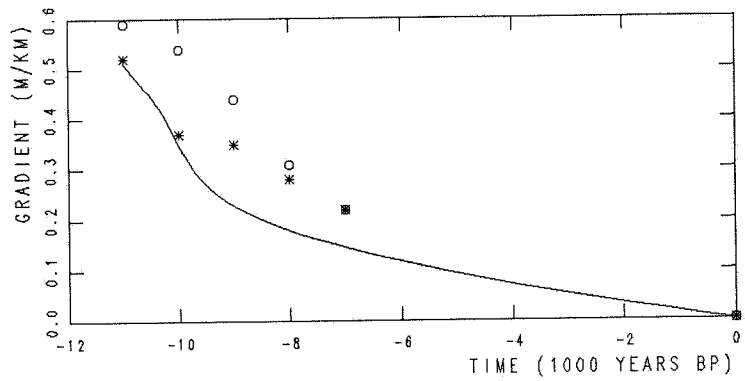

Fig. 17. The observed (solid line; from Svensson, 1989), and theoretical shoreline tilting in Oskarshamn, southern Sweden (location 4 in Fig. 13). The calculations are done for flexural rigidity of 10^{24} and 10^{25} Nm, indicated by stars and dots, respectively.

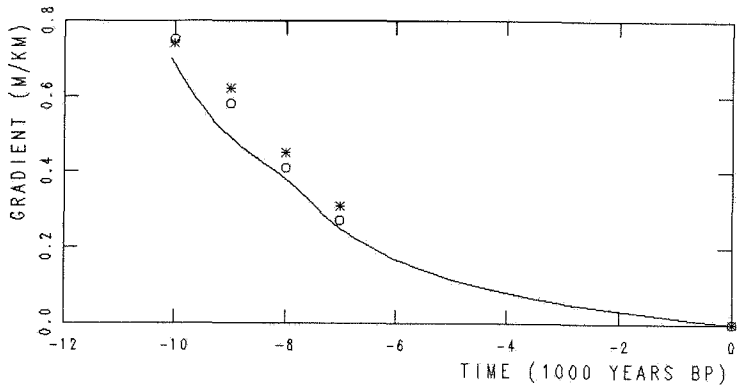

Fig. 18. The observed (solid line; from Donner, 1980), and theoretical shoreline tilting in the Helsinki-Tampere area (location 5 in Fig. 13). The calculations are done for flexural rigidity of 10^{24} and 10^{25} Nm, indicated by stars and dots, respectively.

is equal to or less than 10^{24} Nm, corresponding to a lithosphere thickness $\leq$ 50 km (assuming E = 8.35 x 10^{10} Nm^{-2}). For flexural rigidities greater than 10^{24} Nm a Fennoscandian ice load of the shape generally believed reasonable simply cannot produce the observed strandline tilt at many locations. The mismatch is larger for locations in the western part compared to central parts of the area, which may partly be due to decreasing flexural rigidity towards west.

CONCLUSION

The response of ice-load redistribution on earth models with various mantle viscosities and lithosphere thicknesses is calculated to determine the rheology of the upper parts of the earth.

Based on the observed present rate of uplift and the tilting history of palaeoshorelines in Fennoscandia it is strongly suggested that the earth's mantle is of low viscosity (1.0 x 10^{22} poise) througout (at least down to 1000 km depth). The mantle is capped by a 75 km thick asthenosphere with viscosity 1.3 x 10^{20} poise.

The uplift data further suggests that the lithosphere in the Fennocandian area has a flexural rigidity equal to or less than 10^{24} Nm, corresponding to a mechanical thickness of approximately 50 km (assuming Young's module E = 8.35 x 10^{10} Nm^{-2}). This is at the low end of the 1 to 5 x 10^{24} Nm range suggested by a rough analysis of long term lithospherically-supported gravity anomalies in Fennoscandia (Cathles, 1975). This may be in part due to the fact that most tilt sites are near the present shoreline in a thinner part of the shield. Anyway, the mechanical thickness of the lithosphere does not appear to be increased for short term loads.

REFERENCES

Artyushkov, E. V.(1971) 'Rheological properties of the crust and upper mantle according to data on isostatic movements', J.Geophys.Res. 76, 1365-1390.

Barrell, J., (1914) 'The strength of the earth's crust; Part VI Relations of isostatic movements to a sphere of weakness', J.Geol. 22, 655-683.

Cathles, L.M. (1975) The viscosity of the earth's mantle, Princeton Univ. Press, Princeton, N.J.

Cathles, L.M., (1980) 'Interpretation of postglacial isostatic adjustment phenomena in terms of mantle rheology', in N.A. Mörner (ed.): Earth rheology, isostasy and eustasy. John Wiley & Sons, pp. 11-43.

Daly, R.A. (1934) The changing world of the ice age. Yale Univ. Press.

De Geer, G. (1888), (1890) 'Om Skandinaviens nivåförändringar i södra och mellersta Sverige', Geol. Fören. Stockholm Förhandl. 10, 366-379 & p. 61-110.

Denton,G. H. and T.J. Hughes (1981) The last great ice sheets. John Wiley & Sons.

Donner, J. (1980) 'The determination and dating of synchronous Late Quaternary shorelines in Fennoscandia', in Mörner (ed.): Earth rheology, isostasy and eustasy. John Wiley & Sons, pp. 285-293.

Ekman, M. (1989) 'Impacts of geodynamic phenomena on systems for height and gravity', Bull. Géod. 63, 281-196.

Fjeldskaar, W. and R. Kanestrøm (1980) 'Younger Dryas geoid-deformation caused by deglaciation in Fennoscandia', in Mörner (ed.): Earth rheology, isostasy and eustasy. John Wiley & Sons, pp. 569-574.

Gantmacher, F.R. (1960) The theory of marices. Translated from russian by K.A.Hirsch. Chelsea Publ.Co.

Haskell, N.A. (1935) 'The motion of a viscous fluid under a surface load', Physics 6, p. 265-269.

Jeffreys, H. (1959) The earth, its origin history and physical constitution. Fourth Edition, Cambridge Univ. Press, London and New York.

Kjemperud, A (1982) 'Late Weichselian and Holocene shoreline displacement in parts of Trøndelag, Central Norway'. Dr. Scient. Thesis, Univ. of Oslo, Norway.

Marthinussen, M. (1974) 'Contributions to the Quaternary geology of northeasternmost Norway and the closely adjoining foreign territories, Norges Geologiske Unders. 315, 1-157.

McConnell, R.K. (1968) 'Viscosity of the mantle from relaxation time spectra of isostatic adjustment', J. Geophys. Res. 73, 7089-7105.

Mörner, N.A. (1979) 'The Fennoscandian uplift and Late Cenozoic geodynamics: geological evidence', Geo Journal 33, 287-318.

Niskanen, E. (1949) 'On the elastic resistance of the earth's crust', Ann.Acad.Sci.Finnicae 21: Series A., 1-23.

O'Connell, R.J. (1971) 'Pleistocene glaciation and the viscosity of the lower mantle', Geophys.J.R. astr.Soc. 23, 299-327.

O'Connell, R.J. (1976) 'The effects of mantle phase changes on postglacial rebound', Journ. Geophys.Res. 81, 971-974.

O'Connell, R.J. (1977) 'The scale of mantle convection', Tectonophysics 38, 119-136.

Peltier, W.R. (1974) 'The impulse response of a maxwell earth', Rev.Geophys. and Space Phys. 12, 649-705.

Peltier, W.R. (1980) 'Ice sheets, oceans and the earth's shape', in N.A. Mörner(ed.): Earth rheology, isostasy and eustasy. John Wiley & Sons, pp. 45-63.

Peltier, W.R. (1984) 'The thickness of the continental lithosphere', J. Geophys.Res. 89, 11 303- 11 316.

Svendsen, J.I. and Mangerud, J. (1987) 'Late Weichselian and Holocene sea-level history for a cross-section of western Norway', Journ.Quat.Sci. 2, 113-132.

Svensson, N.-O. (1989) 'Late Weichselian and Early Holocene shore displacement in the Central Baltic, based on stratigraphical and morphological records from Eastern Småland and Gotland, Sweden', Fil. Cand. Thesis, Lund University, Sweden.

Van Bemmelen R.W. and H.P. Berlage (1935) 'Versuch einer mathematischen Behandlung geotektonischer Bewegung unter besonderer Berucksichtegung der Undationstheorie', Beitr. Geophys. 43, 19-55.

Walcott, R.I. (1970) 'Flexural rigidity, thickness, and viscosity of the lithosphere', J.Geophys.Res. 75, 3941-3954.

APPENDIX A

RESPONSE OF A LAYERED NEWTONIAN MANTLE

A1. Fourier-transformed equation of motion

The equation of motion for a viscous medium in the gravity field is:

$$\nabla\cdot\tau + (g_0\ \rho_0\ \nabla\cdot u\ +\ g_0\ u_z\ \partial_z\rho_0)\ z\ =\ 0$$

where
τ = stress
g_0 = gravity
ρ_0 = density
u = displacement
z = unit vector vertical

The last term is the buoyancy arising from the disturbance u_z.
In an incompressible medium with adiabatic density gradients

$$\nabla\cdot\tau = 0 \qquad (1)$$

The Fourier-transform of (1) is

$$ik_x T_{xx} + ik_y T_{xy} + \partial_z T_{xz} = 0$$

$$ik_x T_{xy} + ik_y T_{yy} + \partial_z T_{yz} = 0$$

$$ik_x T_{xz} + ik_y T_{yz} + \partial_z T_{zz} = 0$$

where T is the Fourier transform of τ

A2. Fourier-transformed constitutive relations

For a viscous fluid the constitutive relations are:

I) $$\tau_{kl} = 2\ \eta\ d_{kl}$$

η = viscosity

d_{kl} = deformation

$$d_{kl} = 0.5\ (\ \partial\upsilon_j/\ \partial x_i\ +\ \partial\upsilon_i/\ \partial x_j\ )$$

υ = $\partial u\ /\ \partial t$

Then $$\tau_{kl} = \eta \left(\partial u_j / \partial x_i + \partial u_i / \partial x_j \right)$$

The Fourier-transformed is

$$T_{xz} = \eta\, ik_x v_z + \eta\, \partial_z v_x$$

II) $$\tau_{kk} = \lambda\theta + 2\eta\, d_{kk}$$

where $\theta = \partial v_k / \partial x_k$

v = Fourier-transformed of u

The Fourier-transformed is

$$T_{yy} = \sigma\, ik_y v_y + \lambda\, (ik_x v_x + \partial_z v_z)$$

where $\sigma = \lambda + 2\eta$

A2. Incompressible viscous equations

From the above equations it may be shown that the viscous equations for an incompressible fluid may be written (assuming $k_y = 0$):

$$\partial_z \begin{vmatrix} v_x \\ v_z \\ T_{xz} \\ T_{zz} \end{vmatrix} = \begin{vmatrix} 0 & -ik_x & \eta^{-1} & 0 \\ -ik_x & 0 & 0 & 0 \\ 4\eta k_x^2 & 0 & 0 & -ik_x \\ 0 & 0 & -ik_x & 0 \end{vmatrix} \begin{vmatrix} v_x \\ v_z \\ T_{xz} \\ T_{zz} \end{vmatrix}$$

In non-dimensional form:

$$\partial_z \begin{vmatrix} 2\eta^* ikv_x \\ 2\eta^* ikv_z \\ iT_{xz} \\ T_{zz} \end{vmatrix} = \begin{vmatrix} 0 & 1 & 2\eta^{-1} & 0 \\ -1 & 0 & 0 & 0 \\ 2\eta & 0 & 0 & 1 \\ 0 & 0 & -1 & 0 \end{vmatrix} \begin{vmatrix} 2\eta^* ikv_x \\ 2\eta^* ikv_z \\ iT_{xz} \\ T_{zz} \end{vmatrix} \qquad (2)$$

where η^* is the layer viscosity relative to layer z_{00}.

A3. Propagation technique

Suppose we start with a system of linear, first order differential equation of the form:

$$\partial_z u = A(z)\, u$$

where A is a matrix and u a vector.

This equation gives the rate of change of u at a particular depth. Given a value of u at a particular z, it is clear that we can bootstrap our way up or down to find u at any other level. Here is used a method described by Gantmacher (1960) named "Propagator Matrix Method".

A material whose properties vary continuously as a function of z

may be approximated by one whose properties are constant in thin layers. Assume each layer has a thickness D. If we know u at z=0, we find u at z=1 by using a propagator matrix:

$$u(z_0 + D_1) = e^{A\,(z_0^1)\,D_1}\, u(z_0)$$

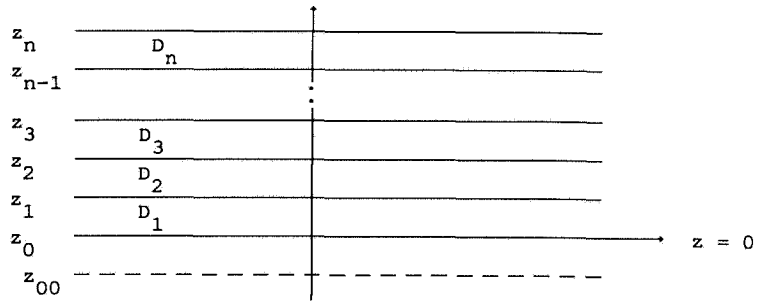

We define a propagator-matrix P_n

$$P_n = e^{A\,(z_{n-1}^n)\,D_n}$$

P_n propagate the solution at the bottom to the top of layer n. The solution at the top of layer n propagated from the bottom layer 00

$$u(z_n) = P_n\, P_{n-1} \cdots\cdots P_3\, P_2\, P_1 \; e^{A\,(z_{00}^0)\,z_{00}}\, u(z_{00})$$

The propagator P for a layer of thickness D , viscosity η (relative to bottom layer) is by (2):

$$P = \begin{pmatrix} CP & C & SP/\eta & S/\eta \\ -C & CM & S/\eta & SM/\eta \\ \eta\,SP & \eta\,S & CP & C \\ -\eta\,S & \eta\,SM & -C & CM \end{pmatrix}$$

where

$$\begin{aligned} S &= kD \sinh kD \\ C &= kD \cosh kD \\ CP &= \cosh kD + kD \sinh kD \\ CM &= \cosh kD - kD \sinh kD \\ SP &= \sinh kD + kD \cosh kD \\ SM &= \sinh kD - kD \cosh kD \\ k &= \text{wavenumber} \end{aligned}$$

The solution at the surface z=n is partly known. We apply a load on top of the n-th layer, so that

$$T_{zz} = -1$$

$$T_{xz} = 0$$

We also find $u(z_0)$ by assuming finite solution in the substratum below z=0, i.e. in z_{00}. This implies that

$$e^{A(z_{00}^{0})\, z_{00}}\, u(z_{00}) = \left(A \begin{pmatrix} 1 \\ 0 \\ 1 \\ 0 \end{pmatrix} + B \begin{pmatrix} 0 \\ 1 \\ 0 \\ 1 \end{pmatrix} \right)$$

The final propagator used in the calculations are:

$$\begin{pmatrix} \sim \\ \sim \\ 0 \\ -1 \end{pmatrix} = P_{NL}\ P_{NL-1}\ P_{NL-2}\ \cdots\ P_3\ P_2\ P_1 \left(A \begin{pmatrix} 1 \\ 0 \\ 1 \\ 0 \end{pmatrix} + B \begin{pmatrix} 0 \\ 1 \\ 0 \\ 1 \end{pmatrix} \right)$$

By propagating the solution at z=0 to the surface and apply the boundary conditions, A and B is uniquely determined, and thus v at the free surface.

The solution is then

$$\begin{vmatrix} 2\,\xi\, ik\, v_x \\ 2\,\xi\, ik\, v_z \\ i\, T_{xz} \\ T_{zz} \end{vmatrix} = \begin{vmatrix} v_1 \\ v_2 \\ v_3 \\ v_4 \end{vmatrix}$$

The relaxation time for the bottom layer is

$$\xi_0 = \frac{2\,\eta_0}{\rho\, g}\, k$$

where η_0 is the viscosity for layer z_{00}

The viscosity varies from one layer to the other, and the relaxation time at the surface is

$$\xi = \xi_0 \,/\, v_2$$

Isostatic compensation as a function of time is

$$h = h_0\, e^{-t/\xi} \qquad (3)$$

h_0 is total isostatic displacement according to (4)

APPENDIX B

LITHOSPHERE FLEXURE

If a load is applied to a fluid, the surface of the fluid will deform until the weight of the fluid displaced from the equilibrium level balances the applied load. If an elastic lithosphere covers the fluid, part of the applied load will be supported by the lithosphere, part by the buoyant forces of the fluid beneath acting through the lithosphere.

Loads of short wavelength are supported by the lithosphere. The lithosphere thus acts as a lowpass filter. The characteristics of this filter depends on the elastic strength of the lithosphere. A measure of the elastic strength of the lithosphere is a parameter called the flexural rigidity, that is the resistance to flexure. The elastic strength of the lithosphere is a function of the mechanical thickness,

and is determined by the following equation :

$$\text{Flexural rigidity} \quad D = \frac{EH^3}{12(1 - \nu^2)}$$

where H = elastic thickness
E = Young's modulus
ν = Poisson's ratio

The regional isostatic compensation is achieved by:

$$h_0 = \frac{F(k)\ \alpha^{-1}}{\rho g} \qquad (4)$$

where F(k) = transformed ice load
ρ = density of the upper mantle
g = gravity

and the "lithosphere filter" α:

$$\alpha = \frac{2\mu k}{\rho g}\ [(S^2 - k^2H^2) + (CS + kH)]/(S + kHC)$$

where k = wavenumber
H = mechanical thickness of the lithosphere
μ = Lame's parameter
S = sinh kH
C = cosh kH

The lithosphere increases the rate of compensation of short wavelengths of load (cfr. (3)):

$$h = h_0\ e^{-t\alpha/\xi} \qquad (5)$$

h_0 is total isostatic displacement according to (4)